3H-UWAC based on SOFAR Plane: A Novel Relay Deployment Technique

Jiajie Xu, *Student Member, IEEE*, Mustafa A. Kishk, *Member, IEEE,* Mohamed-Slim Alouini, *Fellow, IEEE*

***Abstract*—In this paper, to improve the underwater communication capacity at a level of thousands of kilometers, we propose a three-hop underwater wireless acoustic communication (3H-UWAC) structure based on the Sound Fixing and Ranging (SOFAR) channel. The proposed 3H-UWAC consists of transmitters, relay stations (RSs), and receivers. RSs are set on the SOFAR plane at a known depth. The transmitter will send the information to the nearest first relay station (NFRS) on the SOFAR plane with a narrow beam width. Then, the NFRS will send the information to the nearest relay station to the receiver on the SOFAR plane with a narrow beam width, which is the nearest second relay station (NSRS). Tools from stochastic geometry are used to model the spatial distributions of transmitters', receivers', and RSs' locations. The coverage probabilities (CPs) of the three hops (transmitter to FRS, FRS to SRS, and SRS to receiver) are analyzed, and the final CP from a transmitter to a receiver through the 3H link is derived.**

I. INTRODUCTION

With the exploration of undersea resources and the development of underwater technologies, short or medium-range UWAC methods and algorithms have been extended to achieve good performance. Since the underwater acoustic signal propagation path is a curve, the transmitter can only broadcast communication data. Besides that, there are two challenges for underwater long-distance wireless communication (ULWC): 1) Indeterminate sound velocity and sound profile in the underwater environment; 2) Curve propagation of the underwater acoustic signal. Hence, the methods and strategies of normal UWAC can not be used in ULWC.

Based on experiments, A special channel was found, where the acoustic can propagate similar to a line is named **SOFAR Channel** (Sound Fixing and Ranging channel). It is defined as a horizontal layer of water in the ocean at which the speed of sound is at its minimum (it will be called the SOFAR plane in this paper). In the large-scale underwater communication scenario with a critical vertical depth, since the transmitter doesn't know where the receiver is, the transmission is similar to broadcast. To improve energy efficiency, the broadcast-like signal is angled with a beamwidth rather than omnidirectional, and the angle is named vertical directivity angle (VDA) or vertical beamwidth. VDA is defined as the angular width between the axis of the pattern and 3dB down points at the reference distance of 1 m from the source.

Due to the curve propagation, when a transmitter transmits signals with a large VDA, only a tiny part of the acoustic signal rays can be caught by the receiver, and a critical part of the signal will be scattered and reflected by the sea surface and seabed , which causes low energy efficiency. In this paper, the 3H-UWAC is proposed based on the SOFAR plane with a narrow VDA to improve energy efficiency.

II. SYSTEM MODEL

A. *Structure of the 3H-UWAC*

In 3H communication, there are three hops: the transmitter to FRS, FRS to SRS, and SRS to the receiver, and all of the nodes are considered as random points and obey independent Poisson Point Processes (PPPs). To simplify the calculation without losing insights, signal-to-noise (SNR) is analyzed. Three hops' communication distances are shown in Fig. 1.

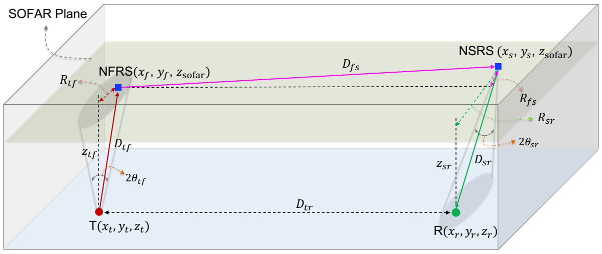

Figure 1: Distances in 3H-UWAC.

B. *CP of the first hop*

Considering the structure of VDA, the distance between the projection of the transmitter on the SOFAR plane and the NFRS, R_{tf}, is less than the coverage radius of the vertical directivity pattern of the transmitter with the VDA of θ_{tf}.

$$\begin{aligned} P_{tf}^{\text{cov}} &= \mathbb{P}\big(\texttt{SNR}_{tf} > \tau, R_{tf} \le z_{tf}\tan(\theta_{tf})\big) \\ &= \mathbb{P}\Big(R_{tf} \le \min\Big(\sqrt{\max\big(\big(\frac{10\lambda}{\alpha_{tf}\ln 10}W\big(\frac{\alpha_{tf}\ln 10}{10\lambda}y_{tf}^{-\frac{1}{\lambda}}\big)\big)^2 - z_{tf}^2, 0\big)}, \\ &\qquad z_{tf}\tan(\theta_{tf})\Big)\Big) \\ &= \int_0^\infty f_{R_{tf}}(r_{tf})\mathbb{1}\big(r_{tf} \le \mathcal{A}\big)\mathrm{d}r_{tf} \end{aligned} \tag{1}$$

where $f_{R_{tf}}(r_{tf}) = 2\gamma_{rs}\pi r_{tf}\exp(-\gamma_{rs}\pi r_{tf}^2)$ is the PDF of the nearest distance in PPP, $y_{tf} = \frac{\tau C_{tf}}{P_{t,tf}}\sigma_{n,tf}^2$, and

$$\mathcal{A} = \min\Big(\sqrt{\max\Big(\big(\frac{10\lambda}{\alpha_{tf}\ln 10}W\big(\frac{\alpha_{tf}\ln 10}{10\lambda}y_{tf}^{-\frac{1}{\lambda}}\big)\big)^2 - z_{tf}^2, 0\Big)}, z_{tf}\tan(\theta_{tf})\Big)$$

C. *CP of the third hop*

The third hop is independent of the first hop, and it is similar to a downlink communication. We can have the Coverage probability of the third hop as follows.

$$\begin{aligned} P_{sr}^{\text{cov}} &= \mathbb{P}\big(\texttt{SNR}_{sr} > \tau, R_{sr} \le z_{sr}\tan(\theta_{sr})\big) \\ &= \mathbb{P}\Big(R_{sr} \le \min\Big(\sqrt{\max\big(\big(\frac{10\lambda}{\alpha_{sr}\ln(10)}W\big(\frac{\alpha_{sr}\ln(10)}{10\lambda}y_{sr}^{-\frac{1}{\lambda}}\big)\big)^2 - z_{sr}^2, 0\Big)}, \end{aligned}$$

$$z_{sr}\tan(\theta_{sr}))\Big)$$

$$= \int_0^\infty f_{R_{sr}}(r_{sr})\mathbb{1}\big(r_{sr} \le \mathcal{B}\big)\mathrm{d}r_{sr} \tag{2}$$

where $f_{R_{sr}}(R_{sr}) = 2\gamma_{rs}\pi r_{sr}\exp(-\gamma_{rs}\pi r_{sr}^2)$ is the PDF of the nearest distance in PPP, $y_{sr} = \frac{\tau C_{sr}}{P_{t,sr}}\sigma_{n,sr}^2$, and

$$\mathcal{B}=\min\Bigg(\sqrt{\max\Big(\big(\frac{10\lambda}{\alpha_{sr}\ln 10}W\big(\frac{\alpha_{sr}\ln 10}{10\lambda}y_{sr}^{-\frac{1}{\lambda}}\big)\big)^2-z_{sr}^2,0\Big)}, z_{sr}\tan(\theta_{sr})\Bigg)$$

D. The second hop from the FRS to the SRS

The top view of the second hop is shown in Fig. 2. D_{fs} means the propagation distance in the second hop. R_{tf} denotes the distance between the projection of the transmitter on the SOFAR plane and the NFRS, which is the nearest distance in a PPP. Similarly, R_{sr} is the distance between the projection of the receiver on the SOFAR plane and the NSRS.

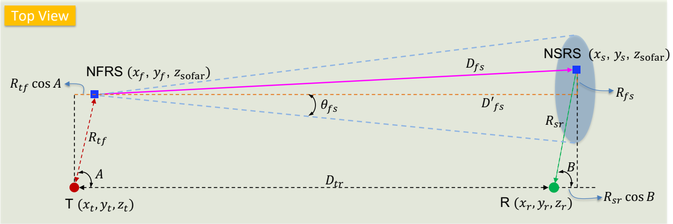

Figure 2: Top view of the second hop.

$$\begin{aligned}
P_{fs}^{\mathrm{cov}} &= \mathbb{P}\big(Successful\,transmission\,from\,NFRS\,to\,NSRS\big|FRS \\
&\qquad and\,SRS\,are\,the\,nearest\,relays\,to\,transmitter\,and\,receiver\big) \\
&=\mathbb{E}_{R_{tf},R_{sr}}\big[\mathbb{P}\big(\mathtt{SNR}_{fs}\ge\tau,R_{fs}\le(D_{tr}-R_{tf}\cos(A)+R_{sr}\cos(B))\tan(\theta_{fs})\big)\big] \\
&=\int_0^\infty f_{R_{tf}}(R_{tf})\int_0^\infty f_{R_{sr}}(R_{sr})\int_0^{2\pi} f_A(a)\int_0^{2\pi} f_B(b) \\
&\quad\times\mathbb{1}\Big(\big(r_{tf}\sin(a)-r_{sr}\sin(b)\big)^2\le\mathcal{C}\big(r_{tf},r_{sr},a,b\big)\Big)\mathrm{d}a\mathrm{d}b\mathrm{d}r_{tf}\mathrm{d}r_{sr},
\end{aligned} \tag{3}$$

wher

$$f_A(a) = \begin{cases}\frac{1}{2\pi}, & 0\le a\le 2\pi\\ 0, & else\end{cases}, \quad f_B(b) = \begin{cases}\frac{1}{2\pi}, & 0\le b\le 2\pi\\ 0, & else\end{cases},$$

$$\begin{aligned}
\mathcal{C}(r_{tf},r_{sr},a,b) = \min\Bigg(&\max\Big(\frac{100\lambda^2}{\alpha_{fs}^2\ln^2(10)}W^2\big(\frac{\alpha_{fs}\ln(10)}{10\lambda}y_{fs}^{-\frac{1}{\lambda}}\big) \\
&- \big(D_{tr}-r_{tf}\cos(a)+r_{sr}\cos(b)\big)^2, 0\Big), \\
&\Big(D_{tr}-r_{tf}\cos(a)+r_{sr}\cos(b)\Big)^2\tan^2(\theta_{fs})\Bigg),
\end{aligned}$$

$y_{fs} = \frac{\tau C_{fs}\sigma_{n,fs}^2}{P_{t,fs}}$, D_{tr} is the distance between the transmitter and the receiver which is known.

E. Total CP of 3H communication

The final CP from the transmitter to the receiver.

$$\begin{aligned}
P_{total}^{\mathrm{cov}} &= \mathbb{E}\big[\mathbb{P}_{tf}^{\mathrm{cov}}{}_{|R_{tf}} \times \mathbb{P}_{fs}^{\mathrm{cov}}{}_{|R_{tf},R_{sr},A,B} \times \mathbb{P}_{sr}^{\mathrm{cov}}{}_{|R_{sr}}\big] \\
&=\int_0^\infty\int_0^\infty\int_0^{2\pi}\int_0^{2\pi} f_{R_{tf}}(r_{tf})f_{R_{sr}(r_{sr})}f_A(a)f_B(b)\mathbb{1}(r_{tf}\le\mathcal{A})\mathbb{1}(r_{sr}\le\mathcal{B}) \\
&\quad\times\mathbb{1}\big(\big(r_{tf}\sin(a)-r_{sr}\sin(b)\big)^2\le\mathcal{C}(a,b,r_{tf},r_{sr})\big)\mathrm{d}a\mathrm{d}b\mathrm{d}r_{sr}\mathrm{d}r_{tf}.
\end{aligned} \tag{4}$$

III. NUMERICAL ANALYSIS AND SIMULATIONS

From Fig. 3(a), we can observe that for different values of z_t, with the increase of z_r, CP will rise to the maximum value gradually. Another point that needs to be marked is all the CPs dropped sharply to 0 when z_r goes to around 6.8 km. According to our exploration of the mathematical calculation, $\mathtt{SNR}$ of the third hop will be less than the threshold τ when the depth of the receiver is greater than 6.8 km. Hence P_{sr}^{cov} will equal 0, and the total CP will go to 0.

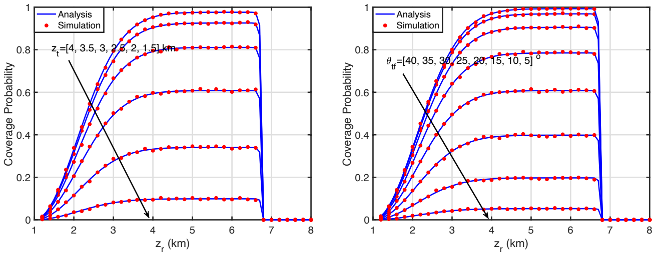

(a) CP varies with depth of the receiver given different depth of the transmitter, $\theta_{tf} = \theta_{sr} = 20°$, and $\theta_{fs} = 5°$. (b) CP varies with VDA of the receiver given different VDAs of the transmitter, $\theta_{fs} = 5°$, $\theta_{sr} = 20°$, and $z_t = 2.5$ km.

Figure 3: CPs vary with different parameters.

Fig. 3(b) shows the different CP performance of different VDA in the first hop, θ_{tf}, with given $z_t = 2.5$ km and z_r varies from 1.2 km to 8 km. It is easy to find that a bigger θ_{tf} achieves a better coverage performance. A bigger VDA in the first hop, θ_{tf}, can cover a greater area on the SOFAR plane at a given depth of the transmitter so that a better CP performance will be achieved in the first hop. In Fig. 4, we change the parameters in the same hop (in the first hop) and identify the effects made by the two factors: (i) the depth of the transmitter and (ii) the VDA. We can see that when z_t is at a lower level, even if θ_{tf} is at a high level, for example, $40°$, the CP is still very small. Similarly, when $\theta_{tf} = 5°$, CP keeps at a low level even with a big z_t (compared with other curves). Comparing Fig. 4(a) and Fig. 4(b) further, we can find that θ_{sr} and z_r in the third hop affect the maximum CP of the system. Again, when z_t ups to 6.8 km, $\mathtt{SNR}$ of the first hop will lower the decoding threshold so that the CP will be 0.

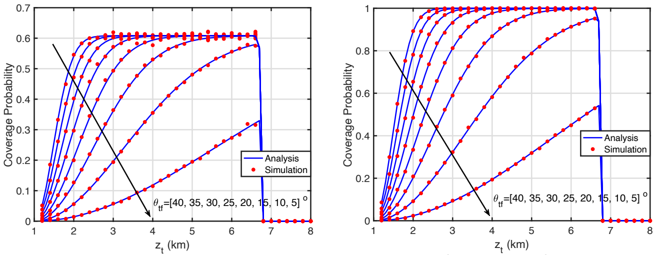

(a) $\theta_{fs} = 5°, \theta_{sr} = 20°, z_r = 2.5$ km (b) $\theta_{fs} = 5°, \theta_{sr} = 40°, z_r = 5$ km

Figure 4: CPs varies with different θ_{sr} and z_r.

IV. CONCLUSION

In this paper, we proposed a 3H-UWAC structure to realize long-distance communication based on the SOFAR channel, where the communication distance can be up to a thousand kilometers. To the best of our knowledge, the proposed 3H-UWAC is the first to study three-hop long-distance underwater communication based on the SOFAR channel.